Physica D 447 (2023) 133688

Contents lists available at ScienceDirect

Physica D

journal homepage: www.elsevier.com/locate/physd

The universal behavior of modulated stripe patterns

Alan C. Newell, Shankar C. Venkataramani *

Department of Mathematics, University of Arizona, 617 N. Santa Rita Ave., Tucson, AZ 85721, USA

ARTICLE INFO

Article history:
Received 28 June 2022
Received in revised form 11 January 2023
Accepted 15 February 2023
Available online 21 February 2023
Communicated by Dmitry Pelinovsky

Keywords:
Pattern formation
Universality
Defects

ABSTRACT

There are three aims of this paper. The first is to explain the reasons for behavior we had long suspected to be true but the real reasons for which we could never quite nail down. Modulated striped patterns arising from a wide class of gradient microscopic pattern forming systems display universal behavior. Their order parameter evolves according to a phase diffusion equation that derives from an averaged energy that consists of coordinate invariant combinations of the coefficients in the metric and curvature two forms of a well-defined phase surface. The evolution towards universality is asymptotic in that the pattern evolves in such a way that, over longer and longer time scales, many terms from the microscopic energy simply become negligible leaving behind canonical forms common to a wide class of microscopic pattern-forming systems. The second aim is to emphasize with some new results the key role that the Jacobian matrix of the map from physical to order parameter space plays in both two and three dimensions. In two dimensions, it is closely related to the Gaussian curvature of the phase surface. It is a conserved density whose integral over space in two dimensions or on cross-sections in three become boundary terms that measure the topological indices of point defects in two dimensions and loop defects in three. In all dimensions, the Jacobian matrix acting on the order parameter vector, the gradient of the phase, is zero when the local pattern wavenumber is close to its preferred value and this leads to the effective linearization of the phase diffusion equation. The third aim is to honor Hermann Flaschka, a close friend and scientific colleague for over fifty years, an outstanding mathematician, a true gentleman and scholar with an uncanny knack of explaining the most complicated of ideas in the simplest of ways, who passed away last year. Hermann was one of the founding editors of Physica D and served as the coordinating editor for almost twenty years.

1. Introduction and general discussion

Natural patterns turn up all over the place in nature and in laboratories. A simple uniform state of a microscopic system driven far from equilibrium by some external stress can destabilize at a certain threshold [1,2]. At that phase transition, various shapes and configurations become preferentially amplified and, via nonlinear interactions, compete for dominance until a new winning and energy minimizing state emerges. In this paper, we focus on a class of gradient microscopic systems that are translationally and rotationally invariant and whose preferred post instability planform is one of stripes or rolls in which the microscopic field breaks translational symmetry and is locally periodic. However, rotational invariance is not broken. In spatial geometries whose size greatly exceeds the local pattern wavelength, the stripe wavelengths l are chosen to within certain bounds, but their orientations are not. Those are chosen by local biases. As a result, the emerging pattern is not a uniform state of stripes all pointing in the same direction but consists of a mosaic of patches of stripes with different orientations that meet and meld together along line and point defects in two dimensions and on planes, lines and points in three.

The underlying microscopic field $w(\vec{x}, t)$ is locally periodic and has the form

$$w(\vec{x}, t) = w(\theta; \nabla\theta = \vec{k}(\vec{X} = \epsilon\vec{x}, T = \epsilon^2 t)) = \sum A_n(k^2)\cos n\theta . \tag{1.1}$$

The phase gradient is modulated over distances L (box size or average distance between defects) that is long with respect to the local wavelength l. The ratio $\epsilon = \frac{l}{L}$, the inverse aspect ratio, is small and we take advantage of this fact. Using asymptotic WKB-like methods derived from the pioneering ideas of Keller [3] and Whitham [4] for slowly modulated oscillators and waves, we can define and describe the evolution of the macroscopic order for such patterns. That order parameter is the phase $\theta(\vec{x}, t)$ of the underlying locally periodic field along with its gradient, the local pattern wavevector $\vec{k}$. The evolution equation has the form [5–7]

$$\tau(k^2)\Theta_T + \nabla \cdot \vec{k}B(k^2) + \epsilon^2\eta\nabla^4\Theta = 0 \tag{1.2}$$

* Corresponding author.
E-mail address: shankar@math.arizona.edu (S.C. Venkataramani).

https://doi.org/10.1016/j.physd.2023.133688
0167-2789/

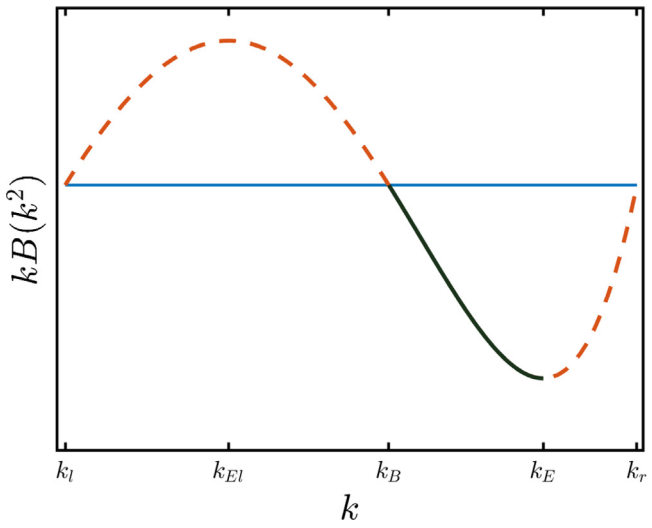

Fig. 1. The universal shape of the function $kB(k^2)$. The solid portion of the curve corresponds to the Busse balloon $k_B < k < k_E$ where the uniform stripe solutions are elliptically stable. The dashed portion corresponds to regions that are unstable to perturbations. To remain well-posed despite these instabilities the phase diffusion equation requires the inclusion of higher order terms that are regularizing.

where $\tau(k^2)$ and η are positive. In (1.1), the microscopic field $w(\vec{x}, t)$ is locally 2π periodic in θ. It is even in θ, reflecting the fact that the contours representing the maxima of w can be labeled $0, 2\pi, 4\pi$ or by their negatives. There are two important consequences of this. First, the gradient of the phase is not a vector field on the plane but rather on its double cover. Thus in general, $\nabla\theta = \vec{k}$ will be a director field and not a vector field on the plane. Second, the microscopic field w can be represented by a cosine Fourier series as shown. In Eq. (1.2), the *phase diffusion equation*, $\theta(\vec{x}, t) = \dfrac{\Theta(\vec{X}, T)}{\epsilon}$, $\vec{X} = \epsilon\vec{x}, T = \epsilon^2 t$, so that $\vec{k}(\vec{X}, T) = \nabla_{\vec{x}}\theta = \nabla_{\vec{X}}\Theta$. The restriction that $\vec{k}$ is only defined as a vector field on the double cover of the plane has consequences as it broadens the number of states into which the pattern may settle. In particular, the canonical point singularities turn out to be disclinations, on contours surrounding which the wave director twists not by integer multiples of 2π but by multiples of π. That twist is proportional to the amount of Gaussian curvature of the phase surface that resides at point singularities.

Although the cubic shape of the function $B(k^2)$ (shown in Fig. 1) was well understood to be universal, the exact nature of the regularization, chosen from special examples to be the biharmonic of Θ and suspected to have that form in general, remained an open challenge. The first new result of this paper is to explain why that is so. We will see that the key idea is that, under the evolution that takes place on the horizontal diffusion time, almost everywhere the local wavenumber tends to a preferred choice dictated by minimizing the energy that governs that evolution. We shall see that energy can be thought of as analogous to the strain energy connected with elastic sheets and its minimization is equivalent to the appearance of and preference for isometric deformations. This fact then removes most of the terms that appear in the correction to the energy leaving only those contributions which can be identified with the bending energy of elastic surfaces. In the pattern context, it is the energy that is stored along line defects and the cost is incurred because the phase contours have to bend across line defects.

Regularization is needed because $\nabla \cdot \vec{k}B$ is a quasilinear differential second order spatial operator on Θ whose matrix of coefficients has eigenvalues B and $\frac{d}{dk}(kB)$ which may, and indeed are, not necessarily negative for all wavenumbers k throughout the pattern. The consequence is that the unregularized Eq. (1.2) is a diffusion equation with negative diffusion coefficients at some locations and therefore, without regularization, is ill posed. Eq. (1.2) can be formally written as

$$\tau(k^2)\Theta_T = -\frac{\delta\overline{E}}{\delta\Theta} \tag{1.3}$$

where

$$\begin{aligned}\overline{E} &= \iint d\vec{X}\left(\left(-\frac{1}{2}\int^{k^2} Bdk^2\right) + \frac{1}{2}\epsilon^2\eta(\nabla\cdot\vec{k})^2\right)\\ \overline{E} &= \frac{1}{2\pi}\int_0^{2\pi} Ed\theta\end{aligned} \tag{1.4}$$

It turns out that $\overline{E}$ is simply the original microscopic energy E averaged over the local periodicity of the pattern; namely $\overline{E} = \dfrac{1}{2\pi}\int Ed\theta$. The question is: Why is it that all the terms in the order ϵ^2 contribution to $\overline{E}$ other than the curvature $(\nabla\cdot\vec{k})^2$ that could arise from averaging the original energy E are negligible and of lower order in ϵ? We shall see when we average E that many other terms are possible. But only the squared mean curvature survives! We shall also see that the Gaussian curvature can also be in the integrand but this integrates out to a boundary contribution that measures the amount of Gaussian curvature that, under the initial evolution described by (1.2), will condense onto and reside at point defects.

The answer is that the non-universal terms are still present for the initial stages of the evolution (1.2). The first part of the evolution that occurs on the horizontal diffusion time scale $T_h = \frac{1}{\epsilon^2}$, the time it takes diffusion to communicate across the macroscopic distance L, will see the pattern attempt to reach a state where the first part of the averaged energy is minimized. That occurs when k tends to a preferred wavenumber k_B that turns out the be the middle zero of the graph of $kB(k^2)$ versus k (See Fig. 1). For pattern forming systems that arise from microscopic gradient flows, the wavenumber k_B is the one chosen by all the various selection mechanisms; minimization of the energy; the edge of the Busse balloon corresponding to the zig-zag stability boundary; circular or curved patterns, stationary dislocations; boundary constraints. For microscopic systems that are not gradient, many features of the phase diffusion equation are the same but the fact that, for example, dislocations do not necessarily remain stationary at k_B, which in the non-gradient case is the zig-zag instability edge of the Busse balloon, means that the apparent gradient structure of the phase diffusion equation is not sufficient to guarantee the pattern macroscopic evolution is gradient. This is why we stipulated that we are at present only treating pattern forming systems that are gradient at the microscopic level.

But given that the underlying microscopic system is gradient, then, almost everywhere, k tends to k_B. But it cannot become k_B everywhere because of boundary constraints and the fact that different neighboring stripe patches have different orientations means that $k < k_B$ along line defects. But almost everywhere on the horizontal diffusion time scale $k^2 - k_B^2$ becomes small. This has two key consequences. First, for times long with respect to T_h, the minimization of the first part of the macroscopic and averaged energy leads to $k^2 - k_B^2$ being small almost everywhere in the averaged energy integration domain. As we shall see, this means that all the potentially non-universal terms that could arise in the second part of $\overline{E}$ become negligible. All derivatives that capture the modulation of the pattern of the form $\vec{k}\cdot\nabla k^2$, that measure the changes of wavenumber normal to the constant phase contours, are much smaller than derivatives such as $\nabla\cdot\vec{k}$ that measure its changes along the phase contours.

In fact, even along phase grain boundaries when $k < k_B$, $\underline{k}$ changes very little in the direction of the local wavevector $\vec{k}$. $\nabla \cdot \vec{k}$ on the other hand measures the curvature of the phase contour and is non-negligible and indeed very important near both line and point defects. The result is that, as the evolution progresses past the horizontal diffusion time, only the terms measuring curvature in what amounts to the Taylor expansion of the original microscopic energy integrand $W(w, \nabla w \cdot \nabla w, \nabla \cdot \nabla w, \ldots)$ with rotational and translational symmetries, $\nabla_{\vec{x}} = \vec{k}\frac{\partial}{\partial \theta} + \epsilon \nabla_{\vec{X}}$ in powers of $\epsilon \nabla_{\vec{X}}$ about the pure periodic state, survive. The average energy does not start out being universal but, as the system evolves, most of the terms that might be present in the microscopic description of the system simply become too small to contribute to the averaged energy $\overline{E}$. Only a canonical subset of the possible terms remains relevant. For pedagogic reasons, we use generic expressions (2.1) and (2.22) for the microscopic energies in our presentation of thes results, so the work falls short of being a rigorous proof. Nevertheless, the expressions used are sufficiently general to persuade a reader of the truth of our assertions.

The second important consequence is that the Hessian $f_x g_y - f_y g_x$, $\vec{k} = (f, g)$ and Jacobian of the map from (x, y) to (f, g) is almost everywhere zero as, except near point and line defects, all x, y points map to the circle $k^2 = k_B^2$. Modulo a factor which becomes constant because k^2 tends to k_B^2, this is also the Gaussian curvature. Thus, under the evolution, the Gaussian curvature of the phase surface, which may initially be distributed, will slowly condense onto line defects. Then, as the line defects evolve so that the corresponding local phase surface has a nonzero curvature in only one direction (across the line defect) and zero curvature in the orthogonal direction, the Gaussian curvature tends to zero on the line defects. But the Gaussian curvature is a conserved density and therefore has no option but to end up condensing onto points. These points often lie at the intersection of the line defects, the most important of which are the concave and convex disclinations. That condensed Gaussian curvature gives rise to the invariant indices that characterize these two canonical point defects of two dimensional patterns. There is also another important outcome of this property of the Jacobian matrix. We shall see that it allows for an almost linearization of the stationary phase diffusion Eq. (1.2) not only in two but in all spatial dimensions. The linearization expresses the fact that, at later times, the evolution is governed by a self-dual approximation in which the small amount of strain energy that survives near defects is balanced by the bending energy contribution there. The obstacle to an exact self-dual behavior is due to the presence of Gaussian curvature of the phase surface localized at points (loops in three dimensions) but their presence can be well approximated by delta function sources whose strengths are known. This is the second new result of this paper.

The outline of this paper is as follows. In Section 2.1, we begin by applying the averaging to a pattern forming system for a complex field with a real valued energy functional which admits very simple spatially periodic solutions $w(\vec{x}, t) = Ae^{i\theta}, \theta = \vec{k} \cdot \vec{x}$. In such cases, the averaging process is extremely simple and the outcomes, and especially the reasons for the emergence of universal behavior, are transparent. In Section 2.2, we apply the ideas to real fields where the locally periodic solutions are not so easily represented but which, nevertheless, lead to the same universal outcomes. In all we do, the phase is the active order parameter and the amplitude (or sequence of amplitudes in the case of real fields) is a passive coordinate slaved to the modulus k of the phase gradient. But there may be places in the pattern, centers of dislocations, amplitude grain boundaries, where the amplitude becomes small and at those places the amplitude is no longer algebraically slaved to k but rather becomes an active order parameter with its own evolution equation. This is also the case near onset. What one must do at such locations remains an open question.

In Section 3, we list many of the properties of solutions of the canonical solutions of the regularized phase diffusion equation and in particular those solutions which capture point and line defects. We raise several important challenges. In Section 3.1, we discuss open questions connected with the energy minimizing convection patterns in elliptical containers with heated horizontal boundaries. Although much of this evolution has been covered in earlier works, there are still several outstanding open questions which we highlight. Principal among the outstanding challenges is the fact that disclinations which form along the major axes between the foci due to the so called nipple instability seem to want to coalesce into dislocations and the final state seems to be close to a multi-dislocation on the principal axis. However, it cannot be only a multi-dislocation with zero Gaussian curvature as the initial Gaussian curvature reflecting the 2π twist of the wave-vector on the boundary has to be included perhaps by disclinations next to the two foci. It is intriguing that the pattern phase gradient starts out as a vector field in forming the eikonal solution, transitions to a director field because of the nipple instability along the axis where the bend of the phase contours becomes too much and then ends up again as a vector field (except not quite everywhere) in order to reach a final energy minimizing state. In Section 3.2, we discuss equally intriguing open questions connected with loop defects in three dimensions which have rather suggestive fractional invariants of $\frac{1}{3}$, $\frac{1}{2}$ and 1.

2. Canonical patterns

2.1. Canonical patterns of complex fields

Consider the system with complex field $w(x, y, t) = u(x, y, t) + iv(x, y, t)$ with the energy functional

$$E = \int \Big((\nabla^2 + k_0^2) w (\nabla^2 + k_0^2) w^* - R w w^* + \frac{1}{2} w^2 w^{*2} + \beta w w^* \nabla w \nabla w^* \Big)\, dx \tag{2.1}$$

For $\beta > 0, R < 0$, $w = 0$ is the only minimum of E. As R increases through zero, the $w = 0$ solution is unstable to a periodic stripe pattern, infinitesimally stable for a range of k to be defined below,

$$w = A(k^2) e^{i\vec{k}\cdot\vec{x}}, \quad A^2(k^2) = \frac{R - (k^2 - k_0^2)^2}{1 + 2\beta k^2}, \quad k = |\vec{k}| \tag{2.2}$$

However, as we have discussed, because of rotational symmetry and resulting degeneracy, the orientation of naturally arising patterns is determined by local biases so that the pattern, instead of being uniform, will consist of patches of stripes of almost constant wavenumber but with directions that change significantly over distances $\frac{l}{\epsilon}$, large compared to the local pattern wavelength. Accordingly we seek to describe the natural pattern as a modulated version of (2.1) as

$$w = A(k^2; \vec{X} = \epsilon \vec{x}, T = \epsilon^2 t) \exp i\theta(\vec{x}, t) \tag{2.3}$$

where

$$\nabla_{\vec{x}} \theta = \nabla_{\vec{X}} \Theta(\vec{X}, T) = \vec{k}(\vec{X}, T) \tag{2.4}$$

The evolution of w and its complex conjugate are given by

$$w_t = -\frac{\delta E}{\delta w^*}, \quad w_t^* = -\frac{\delta E}{\delta w} \tag{2.5}$$

and then

$$\delta E = \frac{\delta E}{\delta w}\delta w + \frac{\delta E}{\delta w^*}\delta w^* = -w_t^*\delta w - w_t\delta w^* \\ = -2A_t\delta A - 2A^2\Theta_t\delta\theta. \tag{2.6}$$

Inserting (2.3) into (2.1) with

$$\nabla_x(A\exp i\theta) = \exp(i\theta)(i\vec{k} + \epsilon\nabla_{\vec{X}})A \\ \nabla_x^2(A\exp i\theta) = \exp(i\theta)(-k^2 + i\epsilon(2\vec{k}\cdot\nabla_{\vec{X}} + \nabla_{\vec{X}}\cdot\vec{k}) + \epsilon^2\nabla_{\vec{X}}^2)A \tag{2.7}$$

We obtain, upon substitution into (2.1) that

$$E = \int\{(k^2 - k_0^2)^2A^2 - RA^2 + \frac{1}{2}A^4 + \beta k^2A^4 + K\}d\vec{x} \\ + i\epsilon\int\{(k_0^2 - k^2)(\vec{k}\cdot\nabla A^2 + \nabla\cdot kA^2) - (k_0^2 - k^2)(\vec{k}\cdot\nabla A^2 + \nabla\cdot kA^2) \\ + \beta A^3(\vec{k}\cdot\nabla A) - \beta A^3(\vec{k}\cdot\nabla A)\} \\ + \epsilon^2\int\{(2\vec{k}\cdot\nabla A + \nabla\cdot\vec{k}A)^2 + 2(k_0^2 - k^2)A\nabla^2A + \beta A^2(\nabla A)^2\}d\vec{x} \tag{2.8}$$

Several observations about (2.8). First, because of the simplicity of the form of the modulated stripe solution, the averaging

$$\overline{E} = \frac{1}{2\pi}\int_0^{2\pi} Ed\theta \tag{2.9}$$

is done automatically. Second, to make sense of the energy integral, a constant K has to be added to ensure convergence because we have not yet specified the behaviors of the pattern at some distant boundary. We show shortly how that constant is determined. Third, although we have written it out, the $O(\epsilon)$ contribution to $\overline{E}$ vanishes as indeed it must since E is real. Although obvious here, it will not be so obvious when we treat patterns with real fields in Section 2.2. Next, we look at the evolution of the amplitude A, namely

$$2A_t = -\frac{\delta\overline{E}}{\delta A} \tag{2.10}$$

Since the time derivative is order ϵ^2 and the variation of the $O(\epsilon^2)$ part of $\overline{E}$ with respect to A gives rise to second spatial derivatives of $\overline{E}$ which again are $O(\epsilon^2)$, the dominant contribution to (2.10) is the algebraic relation

$$0 = 2A\left(\left(k_0^2 - k^2\right)^2 - R + A^2\left(1 + 2\beta k^2\right)\right) \tag{2.11}$$

Only at special points where A is small (dislocation centers) or near onset where A is also small will this term be balanced by $\frac{\partial A}{\partial t}$ and ∇^2A. In that case, it becomes the amplitude part of the Newell–Whitehead–Segel equation [8,9] for striped patterns near onset. In those circumstances, both the amplitude and phase are active order parameters. Far from onset, however, only the phase is an active order parameter and the amplitude is slaved algebraically to the modulus of the phase gradient by (2.11).

$$A^2 = \frac{R - (k^2 - k_0^2)^2}{1 + 2\beta k^2}. \tag{2.12}$$

We note that, because of the presence of the β, the maximum of the amplitude A is not realized at k_0. Neither will it be maximized at the preferred wavenumber k_B. The evolution of the phase is given by

$$A^2\theta_t = -\frac{1}{2}\frac{\delta\overline{E}}{\delta\theta} \quad \text{or} \quad A^2\Theta_T = -\frac{1}{2}\frac{\delta\overline{E}}{\delta\Theta} \tag{2.13}$$

where $\overline{E}$ is now the averaged energy $\bar{E}_0 + \epsilon^2\bar{E}_2$ where, using (2.12),

$$\overline{E_0} = \int E_0d\vec{x} = \int\left(K - \frac{1}{2}(1 + 2\beta k^2)A^4\right)d\vec{x}. \tag{2.14}$$

The maximum of $(1 + 2\beta k^2)A^4$ and the minimum of its negative is how we define k_B, namely

$$\frac{d}{dk^2}\left(1 + 2\beta k^2\right)A^4 = 0. \tag{2.15}$$

To ensure convergence we choose the added constant K to be $\frac{1}{2}(1 + 2\beta k^2)A^4$ estimated at k_B and therefore write

$$\overline{E_0} = \int\frac{1}{2}\left((1 + 2\beta k^2)A^4\right)_{k^2}^{k_B^2}d\vec{x} \tag{2.16}$$

The negative of its variation with respect to θ gives

$$A^2\Theta_T + \nabla_{\vec{X}}\vec{k}B(k^2) = 0 \tag{2.17}$$

where

$$B(k^2) = \frac{d}{dk^2}\left(1 + 2\beta k^2\right)A^4 \tag{2.18}$$

We have already discussed that (2.17) is ill-posed whenever k is outside the Busse balloon $k_B < k < k_E$ and requires regularization. Here k_E is the Eckhaus stability boundary. We focus on the case where $k < k_B$ that occurs near most of the line and point defects. In that case the regularization is provided by the $O(\epsilon^2)$ terms in the averaged energy (2.8). As we see from (2.8), most of the terms reflect their microscopic origins and so, as it stands, the regularization does not look to be universal. But, on closer inspection, we see that, because they all arise from a multinomial Taylor expansion of the original energy integrand in each of its arguments under the action of $\nabla_{\vec{x}} = \vec{k}\frac{\partial}{\partial\theta} + \epsilon\nabla_{\vec{X}}$, the terms either involve differentiating $\vec{k}$ as it changes direction along the phase contour or differentiation of k^2 in the direction of $\vec{k}$. The $\nabla\cdot\vec{k}A^2$ is an example of the former while $\vec{k}\cdot\nabla_{\vec{X}}(A^2)$ is $\frac{dA^2}{dk}\vec{k}\cdot\nabla k^2$ is an example of the latter. But since $\vec{k}\cdot\nabla k^2$or $\vec{k}\cdot\nabla(k^2 - k_B^2)$ is small because, under the minimization of the first part of the averaged energy, $k^2 - k_B^2$ is small almost everywhere and because even along defect lines there is little change in the wavelength along the defect line, all the latter terms are negligible compared to the former. Let us emphasize this. It is not the fact that A^2 is maximum at k_B as it would be for the case of $\beta = 0$, the complex Swift–Hohenberg equation, but the fact that k^2 is almost constant everywhere that makes the non-universal terms negligible. As a consequence, the only surviving terms in the $O(\epsilon^2)$ part of $\overline{E}$ in (2.18) are the ones involving $\nabla\cdot k$. The second part of the averaged energy can then be well approximated by $\epsilon^2\int d\vec{x}A^2(k_B^2)(\nabla\cdot\vec{k})^2$ and that will be common to all averaged energies arising from a very wide class of microscopic systems. The regularized phase diffusion equation then has the universal form

$$A^2(k_B^2)\Theta_T + \nabla\cdot\vec{k}B + \epsilon^2A^2(k_B^2)\nabla^4\cdot\Theta = 0 \tag{2.19}$$

Moreover, for times of the order of and longer than the horizontal diffusion time, we can also approximate $B(k^2$ by $\left(\frac{dB(k^2)}{dk^2}\right)_{k_B^2}(k^2 - k_B^2)$ and its corresponding energy $\overline{E}$ by

$$\overline{E} = \int\left((\frac{d}{dk^2}B(k^2))_{k_B^2}(k^2 - k_B^2)^2 + \epsilon^2(\nabla\cdot\vec{k})^2A^2(k_B^2)\right)d\vec{x} \tag{2.20}$$

By analogy with elastic systems, it is natural to call the first the pattern "strain" and the second the pattern "bending" energy as, respectively, they involve the first and second spatial derivatives

of the deformation, here the phase. We now turn to the case of real fields for which the averaging process is not quite as transparent. At the end of that section/or in Section 3, we also discuss the defect point indices which measure the amount of Gaussian curvature of the phase surface deposited at that point.

2.2. Canonical patterns for real fields

The previous class of examples for complex pattern fields for which the insertion of the locally complex field led to an automatic averaging of the energy functional was useful in that it allowed us see the big picture relatively easily without the complication of more difficult calculations. Nevertheless, guided by that study we now turn to the case of pattern forming systems with real fields and, although more complicated, follow the steps of the earlier analysis. We consider energies of the form

$$E = \int W d\vec{x} \tag{2.21}$$

where W, the integrand, is any rotationally and translationally invariant function of all even combinations of w and its gradients. By including the up down symmetry, W invariant under w into $-w$, we avoid any possibilities of subcritical bifurcations with non-stripe planforms such as hexagons. (Hexagons can still be a viable multimode planform in such systems but they rely on cubic interactions and are much less likely.) For a typical and generic example of (2.21) we consider,

$$E = \int \left\{ \frac{1}{2}\left((\nabla^2+k_0^2)w \right)^2 - \frac{1}{2}Rw^2 + \frac{1}{4}w^4 + \frac{1}{2}\beta w^2(\nabla w)^2 + K \right\} d\vec{x}. \tag{2.22}$$

The energy in (2.22) can be viewed as a generalization of the Swift–Hohenberg energy [10], which is used as a generic model for real fields that form stripe patterns. The evolution of the microscopic field $w(\vec{x}, t)$ is given by

$$w_t = -\frac{\delta E}{\delta w} = -\left(\nabla^2+k_0^2 \right)^2 w + Rw - w^3 + \beta w(\nabla w)^2 + \beta w^2 \nabla^2 w. \tag{2.23}$$

We can find stationary stripe solutions for Eq. (2.23) by substituting $\theta = \vec{k}\cdot\vec{x}$, $w = \sum_n A_n \cos(n\theta)$ yielding a system of coupled nonlinear algebraic equations for the amplitudes A_n. Within a range of $k_l < k < k_r$, that depends on the parameter R, we can solve these equations to get $A_n = A_n(k^2; R)$, $n = 1, 3, 5, \ldots$ with all the even order amplitudes equal to zero, reflecting the up-down symmetry $w \to -w$ of Eq. (2.23). Summing this Fourier series yields an exact stationary solution for striped patterns

$$w(\vec{x}, t) = w(\theta = \vec{k}\cdot\vec{x}; \{A_n(k^2)\}_1^\infty, R) = \sum A_n(k^2; R)\cos n\theta. \tag{2.24}$$

w is clearly 2π periodic in θ. Also, the use of the cosine series to represent w is deliberate. It reflects the fact that the phase contours can be labeled $0, \pm 2\pi, \pm 4\pi, \ldots$. We now seek modulated solutions as

$$\begin{aligned} &w(\vec{x}, t) = w(\theta; \{A_n(k^2)\}, R; \\ &\nabla\theta = \vec{k}(\vec{X} = \epsilon\vec{x}, T = \epsilon^2 t) = \nabla_{\vec{X}}\Theta(\vec{X}, T)) \end{aligned} \tag{2.25}$$

We can find the evolution equations for $\Theta(\vec{X}, T)$ in two ways. The first is by solving Eq. (2.23) with the modulated form for w iteratively and applying solvability conditions arising from the translational invariance of the pattern that means that $\dfrac{dw}{d\theta}$ is a solution of the homogeneous part of the linearized equation for w. The forcing terms in the equations for the iterates arise from the slow variations of all quantities with respect to $\vec{X}$ and T and the condition that they have to be in the range of the linearized equation for the iterates of w gives the evolution equation for the phase $\Theta(\vec{X}, T)$. We choose to use the second way, used in the previous section, which is to substitute the modulated w into the microscopic energy functional (2.22) and average over θ. We obtain then from (2.21) that

$$w_t \delta w = -\delta E \tag{2.26}$$

which, upon averaging over θ, gives

$$\langle w_\theta^2 \rangle \theta_t \delta\theta = -\delta\overline{E}. \tag{2.27}$$

In carrying out the second approach, we still will have to use the equation analogous to (2.12) expressing the amplitudes A_n in terms of the wavenumber $A_n = A_n(k^2)$. This is significantly more involved and less transparent than the case for the complex field where the slaving of the amplitude equation gives the explicit expression (2.12) for $A(k^2)$.

Substitute (2.25) into (2.21) with

$$\begin{aligned} &\nabla_{\vec{x}} \to \vec{k}\partial_\theta + \epsilon\nabla_{\vec{X}} \\ &\nabla_{\vec{x}}^2 \to k^2\partial_\theta^2 + \epsilon(2\vec{k}\cdot\nabla + \nabla\cdot\vec{k})\partial_\theta + \epsilon^2\nabla_{\vec{X}}^2 \end{aligned} \tag{2.28}$$

and so on. For the moment, then, we write

$$\begin{aligned} &\nabla_{\vec{x}} w = \vec{k} w_\theta + \epsilon\nabla_{\vec{X}} w \\ &\nabla_{\vec{x}}^2 w = k^2 w_{\theta\theta} + \epsilon(2k\cdot\nabla + \nabla\cdot\vec{k})w_\theta + \epsilon^2\nabla_{\vec{X}}^2 w \end{aligned} \tag{2.29}$$

But let us understand what the operator $\nabla_{\vec{x}}\cdot$ means when acting on w given by (2.24),

$$\nabla_{\vec{x}} w = \sum_{n\geq 1}\left(-n\vec{k}A_n(k^2)\sin n\theta + \epsilon\frac{dA_n}{dk^2}\nabla_{\vec{X}}k^2\cos n\theta \right) \tag{2.30}$$

The θ derivative acts on the cosines and the slow derivatives act on k^2 through the amplitude dependence on the latter. We now insert (2.29) into (2.22) and average by writing

$$\overline{E} = \frac{1}{2\pi}\int_0^{2\pi} d\theta E \tag{2.31}$$

and obtain

$$\begin{aligned} \overline{E} = &\langle \int \left\{ \frac{1}{2}(k^2 w_{\theta\theta} + k_0^2 w)^2 - \frac{1}{2}Rw^2 \right. \\ &\left. + \frac{1}{4}w^4 + \frac{1}{2}\beta k^2 w^2 w_\theta^2 + K \right\} d\vec{x}\rangle \\ &+ \epsilon\langle \int \left\{ (k^2 w_{\theta\theta} + k_0^2 w)(2\vec{k}\cdot\nabla w_\theta + \nabla\cdot\vec{k}w_\theta) \right. \\ &\left. + \beta w^2 w_\theta \vec{k}\cdot\nabla w \right\} d\vec{x}\rangle \\ &+ \epsilon^2\langle \int \left\{ (k^2 w_{\theta\theta} + k_0^2 w)\nabla^2 w \right. \\ &\left. + \frac{1}{2}(2\vec{k}\cdot\nabla w_\theta + \nabla\cdot k w_\theta)^2 + \beta w^2(\nabla w)^2 \right\} d\vec{x}\rangle \\ &+ o(\epsilon^2) \end{aligned} \tag{2.32}$$

We now want to take the same step as we did with the complex field patterns in that we want to include the dependence of all the amplitudes on k^2 as the amplitudes are slaved to the modulus of the phase gradients. The way we do this is to use Eq. (2.23) for w directly after making the substitutions in (2.28) and keeping all

terms to order ϵ^2. We obtain

$$\begin{aligned}
&k^4 w_{\theta\theta\theta\theta} + 2k^2 k_0^2 w_{\theta\theta} + (k_0^4 - R)w + w^3 - \beta k^2 w w_\theta^2 - \beta k^2 w^2 w_{\theta\theta} \\
&\quad = -w_t - \epsilon \Big\{ (k^2\partial_\theta^2 + k_0^2)(2\vec{k}\cdot\nabla w_\theta + \nabla\cdot k w_\theta) \\
&\quad + (2\vec{k}\cdot\nabla + \nabla\cdot\vec{k})(k^2 w_{\theta\theta\theta} + k_0^2 w_\theta) \\
&\quad - 2\beta w w_\theta(\vec{k}\cdot\nabla)w - \beta w^2(2\vec{k}\cdot\nabla w_\theta + \nabla\cdot k w_\theta) \Big\} \\
&\quad - \epsilon^2 \Big\{ (k^2\partial_\theta^2 + k_0^2)\nabla^2 w + \nabla^2(k^2 w_{\theta\theta} + k_0^2 w) \\
&\quad + (2\vec{k}\cdot\nabla + \nabla\cdot k)^2 w_{\theta\theta} \\
&\quad - \beta w(\nabla w)^2 - \beta w^2\nabla^2 w \Big\} + o(\epsilon^2)
\end{aligned} \tag{2.33}$$

Multiply (2.33) by $\frac{1}{2}w$ and average, liberally using integration by parts, to obtain

$$\begin{aligned}
&\frac{1}{2}k^4\langle w_{\theta\theta}^2\rangle - k^2 k_0^2\langle w_\theta^2\rangle + \frac{1}{2}(k_0^4 - R)\langle w^2\rangle + \frac{1}{2}\langle w^4\rangle + \beta k^2\langle w^2 w_\theta^2\rangle \\
&\quad = -\frac{1}{2}\langle w w_t\rangle - \frac{1}{2}\epsilon \Big\{ \langle w(k^2\partial_\theta^2 + k_0^2)(2\vec{k}\cdot\nabla w_\theta + \nabla\cdot\vec{k} w_\theta)\rangle \\
&\qquad \langle w(2\vec{k}\cdot\nabla + \nabla\cdot k)(k^2 w_{\theta\theta\theta} + k_0^2 w_\theta)\rangle \\
&\qquad -2\beta\langle w^2 w_\theta(k\cdot\nabla)w\rangle - \beta\langle w^3(2\vec{k}\cdot\nabla + \nabla\cdot\vec{k})w_\theta\rangle \Big\}
\end{aligned} \tag{2.34}$$

Substitute (2.34) into (2.32) and write

$$\bar{E} = \langle E\rangle = \bar{E}_0 + \bar{E}_1 + \bar{E}_2 \tag{2.35}$$

We will analyze each contribution in turn. First, we observe that the substitution of the amplitude dependence on k^2 manifests as a replacement of the many of the higher derivative terms in the original averaged energy. We find,

$$\bar{E}_0 = \int dxdy \left\{ -\frac{1}{4}\langle w^4\rangle - \frac{1}{2}\beta k^2\langle w^2 w_\theta^2\rangle + K \right\} = \int dxdy E_0 \tag{2.36}$$

The minimum of $\bar{E_0}$ is achieved for $k^2 = k_B^2$ where

$$\frac{d}{dk^2}E_0 = \frac{d}{dk^2}\left(\frac{1}{4}\langle w^4\rangle + \frac{1}{2}\beta k^2\langle w^2 w_\theta^2\rangle \right) = 0 \tag{2.37}$$

where E_0 is the integrand of $\bar{E}_0$. As before, we choose the 'convergence' constant K to be the value of E_0 in the far field where we choose k to be the preferred wavenumber k_B. Thus,

$$E_0 = \left(\frac{1}{4}\langle w^4\rangle + \frac{1}{2}\beta k^2\langle w^2 w_\theta^2\rangle \right)^{\frac{k_B^2}{k^2}} \tag{2.38}$$

Note the similarity between this expression and (2.16). While the numerical coefficients are different, they have the same form if we simply use the first harmonic approximation $w = A_1(k^2)\cos(\theta)$. Consequently, the phase diffusion equation to leading order, obtained from Eq. (2.38), is similar in form to (2.17), and is given by

$$\langle w_\theta^2\rangle\Theta_T + \nabla_{\vec{X}}\vec{k}B(k^2) = 0, \tag{2.39}$$

where

$$B(k^2) = -2\frac{dE_0}{dk^2}. \tag{2.40}$$

We next look at the order ϵ contributions to the averaged energy which, in the case of the complex field, clearly vanished. In the real field case, they still vanish but it takes a little more work to show that they do. The contributions come from two sources, first the terms at $O(\epsilon)$ in (2.32) and second from (2.34) that arose when we effectively replaced the amplitude dependence of the $A_n(k^2)$ sequence. The totality of terms at this level is then given by

$$\begin{aligned}
&\int \Big\{ \langle (k^2 w_{\theta\theta} + k_0^2 w)(2\vec{k}\cdot\nabla w_\theta + \nabla\cdot k w_\theta)\rangle \\
&\quad + \beta\langle w^2 w_\theta\vec{k}\cdot\nabla w\rangle \Big\} d\vec{x} \\
&\quad - \frac{1}{2}\langle w w_t\rangle - \frac{1}{2}\int \Big\{ \langle w(k^2\partial_\theta^2 + k_0^2)(2\vec{k}\cdot\nabla w_\theta + \nabla\cdot\vec{k} w_\theta)\rangle \\
&\quad + \langle w(2\vec{k}\cdot\nabla + \nabla\cdot k)(k^2 w_{\theta\theta\theta} + k_0^2 w_\theta) - 2\beta w^2 w_\theta\vec{k}\cdot\nabla w\rangle \\
&\quad - \beta\langle w^3(2\vec{k}\cdot\nabla + \nabla\cdot k)w_\theta\rangle \Big\} d\vec{x}
\end{aligned} \tag{2.41}$$

The $\langle w w_t\rangle$ term can be written as $\langle w w_\theta\theta_t\rangle = \epsilon\langle w w_\theta\rangle\Theta_T$ which is the average of a perfect theta derivative of a periodic function and therefore zero. All the terms proportional to $\nabla\cdot\vec{k}$ also vanish for the same reason. Likewise, all the terms proportional to k_0^2 vanish. Next we have all the higher derivative terms which we write as

$$\langle 2k^2 w_{\theta\theta}(\vec{k}\cdot\nabla)w_\theta\rangle - \langle k^2 w\partial_\theta^2(k\cdot\nabla)w_\theta\rangle - \langle w\vec{k}\cdot\nabla k^2 w_{\theta\theta\theta}\rangle \tag{2.42}$$

The last two terms can be integrated by parts to give $2k^2 w_\theta(\vec{k}\cdot\nabla w_{\theta\theta})$ which, when added to the first term is $2k^2\vec{k}\cdot\nabla\langle w_\theta w_{\theta\theta}\rangle$ which integrates to zero as w and its derivatives are all periodic. It is remarkable that in the $\beta = 0$ limit that the inclusion of information of how the amplitudes depend on k^2 makes all the terms vanish simply by reason of the periodicity of w.

The terms proportional to β require slightly more work. Their vanishing is not as obvious. The term proportional to $\nabla\cdot\vec{k}$ clearly is a perfect derivative but the other remaining terms combine to give $-\beta\langle w^2 w_\theta(\vec{k}\cdot\nabla)w\rangle$. To see that this is zero, we must remind ourselves that $\vec{k}\cdot\nabla_{\vec{X}}$ acting on w acts only on k^2 through the amplitudes $A_n(k^2)$. Namely $\vec{k}\cdot\nabla_{\vec{X}}w = \sum(\vec{k}\cdot\nabla_{\vec{X}}k^2)\frac{dA_n(k^2)}{dk^2}\cos(n\theta)$. The product of this with the former terms give terms which are all of the form $\cos(r\theta)\cos(s\theta)\sin(m\theta)\cos(n\theta)$ where r, s, m and n are integers and these combine to give sines of four arguments of the form $\sin(\pm r \pm s \pm m \pm n)$ which, if the integrand is not zero integrates to a periodic function and, even if zero, are exactly zero. Therefore, just as in the complex field case, all the $O(\epsilon)$ terms in the averaged energy vanish.

Finally we compute the $O(\epsilon^2)$ contribution. As we have already argued, all terms involving $(\vec{k}\cdot\nabla_{\vec{X}})$ acting on the amplitude sequence give terms proportional to $\frac{dA_n(k^2)}{dk^2}$ times $\vec{k}\cdot\nabla_{\vec{X}}(k^2)$ which we might also write as $\vec{k}\cdot\nabla_{\vec{X}}(k^2 - k_B^2)$. By virtue of the fact that the strain part of the energy makes k^2 close to k_B^2 almost everywhere, these terms are negligible compared to the terms proportional to $\nabla\cdot\vec{k}$. The latter come from both (2.32) and (2.33) respectively as

$$\begin{aligned}
&\epsilon^2\int\frac{1}{2}(\nabla\cdot\vec{k})^2\langle w_\theta^2\rangle d\vec{x} \\
&-\epsilon^2\int\frac{1}{2}(\nabla\cdot\vec{k})^2\langle w w_{\theta\theta}\rangle d\vec{x}
\end{aligned} \tag{2.43}$$

which, after integration by parts, give

$$\epsilon^2\int\langle w_\theta^2\rangle(\nabla\cdot\vec{k})^2 d\vec{x} \simeq \epsilon^2\langle w_\theta^2\rangle_{k_B}\int(\nabla\cdot\vec{k})^2 d\vec{x} \tag{2.44}$$

The regularized phase diffusion equation is then

$$\langle w_\theta^2\rangle \Theta_T + \nabla\cdot \vec{k}B(\vec{k}) + 2\epsilon^2\langle w_\theta^2\rangle \nabla^4\Theta = 0, \tag{2.45}$$

where $\langle w_\theta^2\rangle$ is evaluated at k_B and with

$$B(k^2) = -2\frac{dE_0}{dk^2}, \tag{2.46}$$

where

$$E_0(k^2) = \langle \frac{1}{4}\langle w^4\rangle + \frac{1}{2}\beta k^2\langle w^2 w_\theta^2\rangle\rangle_{k^2}^{k_B^2}, \tag{2.47}$$

which is universal. Although we have carried out the calculation using a typical integrand W for the microscopic energy, it is not hard to see that as long as that integrand is rotationally and translationally invariant with respect to Euclidean transformations and that W is even in the field w, the same arguments will obtain.

3. Two challenges

3.1. The Jacobian of the map from $\vec{x}$ to $\vec{k}$; self-dual reduction of the RCN equation in two, three and any number of spatial dimensions; some properties of defects; and a challenge.

We have seen that the minimization of the strain energy on the horizontal diffusion time scale leads to the local wavenumber k being close to k_B almost everywhere. This fact leads to the elimination of many of the terms that potentially appear in the bending energy and results in the averaged energy being universal. But it also has other consequences. In two space dimensions, the determinant J of the Jacobian $\hat{J}$ of the map from physical space to order parameter space is simply the determinant of the Hessian (i.e. Hessian curvature) $f_x g_y - f_y g_x$. The fact that finite areas of points in physical space map to a circle in order parameter space means that almost everywhere the Hessian and Gaussian curvature of the phase surface are zero. We had previously shown [11] that this allowed us to effectively linearize the regularized phase diffusion equation in two space dimensions. A similar reduction is actually possible in any number of spatial dimensions. A new result is: if k tends to k_B almost everywhere, then differentiation of $\vec{k}\cdot\vec{k} = k_B^2$ with respect to each of the spatial variables gives us that $\hat{J}\vec{k} = 0$. The Jacobian matrix $\hat{J}$ has an eigenvector $\vec{k}$ with an eigenvalue zero. It also means that the determinant is zero but it is the fact that $\hat{J}\vec{k}$ is a zero vector that leads to effective linearization.

The RCN stationary phase diffusion equation is

$$\eta\nabla^4\theta + \nabla\cdot\vec{k}B = -\frac{\delta\overline{E}}{\delta\theta} = 0 \tag{3.1}$$

where

$$\overline{E} = \int\left(\frac{1}{2}\eta|\nabla^2\theta|^2 + \frac{\alpha}{2}G^2\right)d\vec{x} \tag{3.2}$$

and

$$G^2 = -\frac{1}{\alpha}\int_{k_B^2}^{k^2} B dk^2, \quad \alpha = -\frac{1}{2}\frac{dB}{dk^2}\Big|_{k^2=k_B^2} \tag{3.3}$$

The variational derivative of the first term in (3.2) gives rise to the $\eta\nabla^4\theta$ term in (3.1). The variational derivative of the second term is $\frac{\alpha}{2}\frac{dG^2}{dk^2}\cdot 2\vec{k}\cdot\delta\vec{k} = -B(k^2)\vec{k}\cdot\nabla\delta\theta$, which, after integration by parts, is $\nabla\cdot(\vec{k}B(k^2))\delta\theta$, leading to the second term in (3.1). α is a positive "normalizing" constant that is determined by requiring that $G^2 = (k^2 - k_B^2)^2$ at leading order, a fact we will use shortly when we "almost" linearize (3.1).

The energy functional $\overline{E}$ is a generalization of the Aviles–Giga functional [12] and reduces to it for $(k^2 - k_B^2)$ small. As we have indicated, the analysis of this system can be greatly simplified by a self-dual reduction $\sqrt{\alpha}G = \pm\sqrt{\eta}\nabla^2\theta$, and almost everywhere be effectively linearized in any number of spatial dimensions. Self-dual refers to the fact that solutions of the second-order equation $\nabla^2\theta = \pm\sqrt{\frac{\alpha}{\eta}}G$, in which the strain and bending energy contributions balance, also satisfy (3.1). The fact that the linearization is not exact is due to the condensation of nonzero minors of the Jacobian matrix, which in two dimensions is the determinant of J and effectively the Gaussian curvature, onto points in two dimensions and loops in three. These act as localized delta function-like sources in what is otherwise a linearized system. Their influence, however, can be handled in a perturbative manner.

But first, some preliminaries. In two dimensions, a direct calculation shows that, the determinant of the Hessian is a conserved density and its evolution towards localization is described by

$$\tau(k_B)\frac{\partial J}{\partial t} + \nabla\cdot\vec{K} = 0 \tag{3.4}$$

where

$$\vec{K} = (Q_x g_y - Q_y g_x, Q_y f_x - Q_x f_y) \tag{3.5}$$

and

$$Q = (fB)_x + (gB)_y + \eta\nabla^4\theta \tag{3.6}$$

Next, we list some useful formulae that relate the area of the Hessian to a boundary integral and the topological indices associated with the concentration of this quantity at defect points. Similar indices will be associated with closed loops in three dimensions. We will discuss the two dimensional case first. The key formulae are:

$$\begin{aligned}(1-r)F_r + k_B^2 r F_{r+1} &= \int_C \frac{fdg - gdf}{(k_B^2 + f^2 + g^2)^r} \\ &= \int_C \frac{k_B^2}{(2k_B^2)^r}d\varphi = \frac{k_B^2}{(2k_B^2)^r}[\varphi]\end{aligned} \tag{3.7}$$

where $(f,g) = (k\cos\varphi, k\sin\varphi)$, and we assume k is k_B everywhere on the boundary C and $[\varphi]$ is the twist T of the director field $\vec{k}$ as it travels along the boundary circumscribing the area Ω. The function F_r is

$$F_r = 2\int_\Omega \frac{f_x g_y - f_y g_x}{(k_B^2 + f^2 + g^2)^r}dxdy. \tag{3.8}$$

These formulae follow from Green's theorem. In deriving (3.4), we think of the surface as being the dimensional phase surface $z = \frac{\theta}{k_B}$. The formulae can also be used for any r value although the ones which are integer or half integer are the most interesting. For $r = 0$, we obtain

$$F_0 = 2\int_\Omega (f_x g_y - f_y g_x)dxdy = k_B^2 T \tag{3.9}$$

The boundaries can be distant or they can simply be curves surrounding individual defect points such as concave and convex disinclination as long as the first stage of the energy minimization has taken place so that the Hessian has condensed onto points and the wavenumber k is k_B on the circumscribing boundary.

We are now in a position to explain why it is that, for patterns which are locally stripe and planar in any number of spatial dimensions, the stationary RCN equation describing the energy minimizing configurations, including those with line and point defects, can be "almost" linearized. Although much of this conclusion had been conjectured in earlier papers, we now see how dramatic the consequences of the local wavenumber approaching k_B almost everywhere are.

We want to solve (3.1). We ask that if the self-dual or anti self-dual balance of the energies in (3.2) can lead to solutions of (3.1). This hope was originally motivated by an observation that the shape of a stationary dislocation, originally given in [13] and described by the fourth order stationary RCN equation [11], could be described by equating the strain and bending energies in (3.2). It was proven for two dimensional patterns that, if J is identically zero, the same result obtains.

We now show it will hold in any number of spatial dimensions. We set,

$$\nabla^2\theta = \beta s G + s\chi \tag{3.10}$$

where

$$\beta = \sqrt{\frac{\alpha}{\eta}}, \quad s = \pm 1 \tag{3.11}$$

and derive the equation for the amount of χ by which the self-dual and anti self-dual balances do not satisfy (3.1). After a little manipulation, we find, for any number of spatial dimensions that

$$\nabla^2\chi + \nabla s\chi\nabla_{\vec{k}}G = -\beta s\nabla_{\vec{k}}\cdot\left(\hat{J}(\hat{J} - \nabla^2\theta I)\nabla_{\vec{k}}G\right) \tag{3.12}$$

But, since $\nabla_{\vec{k}}G$ is $2\dfrac{dG}{dk^2}\vec{k}$ and, if k^2 tends to k_B^2, $\vec{k}$ is an eigenvector of the Jacobian matrix $\hat{J}$ with eigenvalue zero, the right hand side of (3.12) is zero almost everywhere in the pattern domain. We have seen (see [11]) that, as the pattern evolves, the Gaussian curvature, initially broadly distributed, condensed first onto line defects and then onto points in two dimensions. In general, it concentrates at codimension two defects, so it is only nonzero at point defects in two dimensions, line defects in three.

But we can go further than simply exploiting self-dual solutions. We can almost linearize the equation pair (3.10) and (3.12) in the sense that we can perturbatively solve the pair of Eqs. (3.10) and (3.12) by alternately solving for θ in (3.10) with χ given and for χ in (3.12) with θ, and hence $\hat{J}$ given. This procedure can be implemented by solving linear equations with known forcing terms at each step.

We first focus on the two space dimension case. In that case, as we have shown in [11], the right hand side of (3.12) is $\beta s J\nabla_k^2 G$ where $J = \det(\hat{J})$ is the determinant of the Hessian matrix $f_x g_y - f_y g_x$ which is almost everywhere zero because the map from almost all points (x, y) is to a circle $k^2 = k_B^2$ in order parameter space. Then,

$$\nabla^2\chi + \nabla s\chi\nabla_{\vec{k}}G = \beta s J\nabla_k^2 G. \tag{3.13}$$

Typically, following the behavior of the fundamental solution for the Poisson equation, i.e. the Newtonian potential, the resulting χ will decay as $\dfrac{1}{r}$, $r = \sqrt{x^2 + y^2}$, the distance from point defects where J is located. But, as we have shown, G^2 can be well approximated by $(k^2 - k_B^2)^2$. Since, the sign s takes care of the plus–minus ambiguity, (3.10) becomes

$$\nabla^2\theta = \beta s(k_B^2 - k^2) + s\chi \tag{3.14}$$

Let $\theta = \dfrac{1}{\beta s}\ln\psi$ and find that

$$\nabla^2\psi - (\beta^2 k_B^2 + \beta\chi)\psi = 0 \tag{3.15}$$

Set $\chi = \psi v$ and then v satisfies

$$\nabla^2 v - (\beta^2 k_B^2 + \beta\chi)v = -4\beta\psi^{-1}J \tag{3.16}$$

These equations are valid in the entire two dimensional pattern domain. Clearly if $J \equiv 0$, $\chi = 0$ and (3.15) is linear. Even if J is delta function like, χ decays away from the defect and the equation pair (3.15), (3.16) can be handled perturbatively.

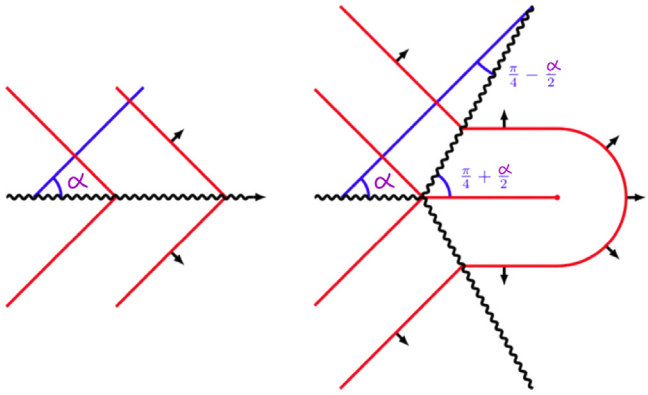

Fig. 2. The nipple instability and the birth of a VX pair.

We now briefly list some of the various solutions of (3.15), (3.16) that correspond to two dimensional defects and some of their key properties. After this brief list, we pose an open challenge.

1. The simplest solutions for which $J \equiv 0$ are sums of exponentials

$$\psi = \sum_1^N \exp(\beta\vec{k}_j\cdot x),\ |\vec{k}_j| = k_B \tag{3.17}$$

$N = 1$ corresponds to a field of straight parallel rolls.

2. The phase grain boundary (PGB) arises when $N = 2$ and leads to a wave vector field

$$\vec{k} = \nabla\theta = \frac{s}{\beta}\frac{\nabla}{\psi}\psi = \frac{1}{2}(\vec{k}_1 + \vec{k}_2) + \frac{1}{2}s(\vec{k}_1 - \vec{k}_2)\tanh\frac{1}{2}(\vec{k}_1 - \vec{k}_2)\cdot\vec{x} \tag{3.18}$$

which is also the weak solution with the usual Maxwell rule for the hyperbolic system $\nabla\cdot\vec{k}B = 0$, $\nabla\times\vec{k} = 0$ when $|\vec{k}| \le k_B$. One can verify by direct computation that $J \equiv 0$.

3. Creation of VX pairs – the nipple instability. If α is the angle that each of the stripe patches makes with the PGB direction, the energy per unit length of PGB is $\dfrac{4}{3}\eta k_B^3\sin^3(\alpha)$. But as $\alpha \to \dfrac{\pi}{2}$, the stripe patches are parallel and there should be no energy cost. This suggests that as α increases, the PGB becomes unstable. It does so to a perturbation in which the former wavevector field of (3.18) becomes a director field. (See the second part of Fig. 2) A VX pair with energy per unit length of the former PGB of $\dfrac{4}{3}\eta k_B^3(1 - \sin(\alpha))$ is created. Thus, PGBs are unstable to concave–convex disclination pairs when $\sin^3\alpha > 1 - \sin\alpha$ or $\alpha \ge 43°$.

4. The canonical point defects, concave (V), and convex (X) disclinations are shown in Fig. 3.

The concave disclination consists of a triad of PGB's meeting at the point defect at 120° angles. The convex disclination consists of a semicircular arc joining straight stripes. Their corresponding phase surfaces have Gaussian curvature localized at the defect points [11]. Their far fields are described by a solution of the Helmholz Eq. (3.17).

5. The far fields of other point defects such as spines, saddles, targets, and vortices which are composites of the canonical point defects V and X can also be captured using the reduction (3.15), (3.16).

6. A particularly interesting defect is the stationary dislocation. It is the composite of a saddle (VV) and a vortex (XX) whose

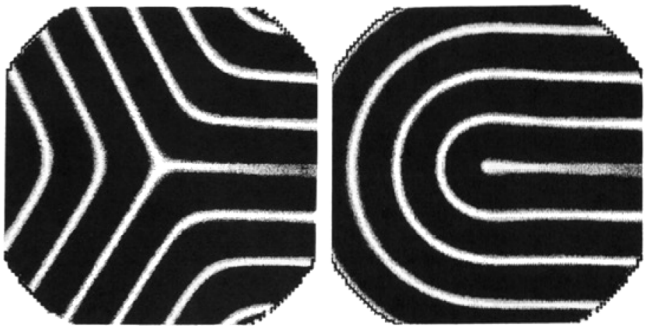

Fig. 3. A concave (left) and a convex (right) disclination.

harmonic (i.e. solutions of $\nabla \cdot \vec{k} = \nabla \times \vec{k} = 0$) structure is given by $f - ig = k_B + \frac{i}{z}$. For a nontrivial $B(k^2)$, their far field is given by seeking solutions $\psi = \exp(\beta k_B x) F(x, y)$ and treating y derivatives of F as more important than x derivatives (the paraxial approximation) so that $F(x, y)$ satisfies $2\beta k_B F_x + F_{yy} = 0$ We seek solutions such that $\theta(-x, y) = \theta(x, y)$ and that $\theta(x, y) = k_B x$ for y large and positive and to $k_B x + \pi \operatorname{sgn}(x)$ for y large and negative. The solution then is

$$\theta(x, y) = k_B x + \frac{1}{\beta} \ln \left\{ \frac{1}{2}(1 + \exp(\beta\pi \operatorname{sgn}(x))) + \frac{1}{2}(1 - \exp(\beta\pi \operatorname{sgn}(x))) \operatorname{Erf}(\sqrt{\beta k_B} \frac{y}{\sqrt{|x|}}) \right\} \tag{3.19}$$

It is not difficult to check that the determinant of the Hessian, $\theta_{xx}\theta_{yy} - \theta_{xy}^2$, and the Gaussian curvature are small for dislocations so that the self dual approximation gives an accurate representation of their shapes. The multi-dislocation state is captured by superpositions of the profile in (3.19) as long as the centers are well separated.

And now we come to our first challenge which we shall introduce through a series of figures. Fig. 4 is the result of a computation of solutions of the Swift–Hohenberg equation with boundary conditions chosen to force stripes meeting at various angles shown across the top of the figure. As predicted in item 3 above, the VX pair creation is beginning to show at 0.25π. It becomes more pronounced as the angle increases and leads to a sequence of such pairs along the PGB. However, we note that the contours emanating from the V become less Y-shaped and more V-shaped so that the arms become more or less parallel to the original PGB itself. Indeed at angles of $.45\pi$, the pattern looks more and more like a sequence of dislocations. This observation is consistent with what we see in ellipses with boundary conditions (in the context of convection in an elliptic cylinder with heated sidewalls) chosen to ensure that the boundary phase contours are parallel to the boundary and the wavevector normal. These are shown in Figs. 5, 6, 7, 8, 9, 11a–b, 12a–b.

In Fig. 5, we see the eikonal solution (namely the solution obtained by moving along boundary normals with phases $0, 2\pi$, etc. marked at intervals of $\frac{2\pi}{k_B}$) regularized by a PGB between the two foci. This would indeed be the solution for an idealized elastic blister whose energy is very similar to (3.2) with carefully controlled boundary conditions. The surface height would rise with a constant slope and meet in a ridge located between the two foci where the cavities begin.

However, one observes that the angles at which the phase contours meet the PGB become larger and larger. Fig. 6 shows us what happens. The white triangle marks the focus, the center of curvature of the end of the boundary along the major axis. The white diamond marks the point at which the angle reaches its critical value and from that point to the center we see a sequence of dislocations with the contours closest to the major axis parallel to that rather than being shaped as they would if they followed the eikonal solution exactly. But as Fig. 7 indicates, the deviation from k_B (here chosen to be unity) is very small and well within the $k - k_B = O(\epsilon)$ tolerance. There are no fitting parameters in Fig. 7 and the grayscale is logarithmic, to highlight small deviations $k - k_B$. It is therefore remarkable that the deviation is really small over the bulk of the domain. Indeed, even a small difference between the nominal k_B from the PDE (the parameter k_0) and the "actual" k_B realized by the solution will show as a bright region in this plot. Fig. 8 shows the local energy density which is clearly largest on the sequence of VX pairs near the foci and on the sequence of dislocations nearer the center of the ellipse. Fig. 9 is a repeat of Fig. 6 with a 4:1 aspect ratio with results very close to that of Fig. 6. Fig. 10 is the result of a simulation of the Oberbeck–Boussinesq equation at a Prandtl number of 100 (at which the equations are almost but not exactly gradient) and a Rayleigh number of 2000. Figs. 11a and 11b are, respectively, the results of an experiment by Meevasana and Ahlers [14] with ethanol and a simulation of Swift–Hohenberg in an identical geometry [15]. Fig. 12a, b are simulations of Swift–Hohenberg [15].

Fig. 4. Numerical solutions of the Swift–Hohenberg equation with boundary conditions corresponding to stripes with increasing angles.

The challenge is to deduce all this structure from the stationary phase diffusion (3.1) for the energy minimizing field. In the far-field, away from the major axis between the foci, the Gaussian curvature (Hessian) would appear to be so small as to be negligible so it is likely the self-dual approximation obtains. On the outside, the mean curvature is also small so the eikonal solution dominates.

But as we move in, the curvature of the phase contours is slightly more pronounced as to allow, if in balance with the strain energy, proportional to $(k^2 - k_B^2)^2$, small deviations in the latter in which $k > k_B$ but well within the Busse balloon and still of order

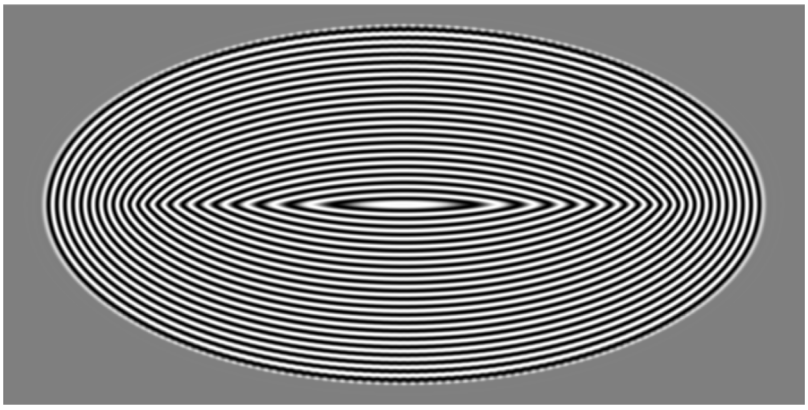

Fig. 5. A stripe pattern corresponding to a phase given by the eikonal equation $|\nabla\theta| = 1$.

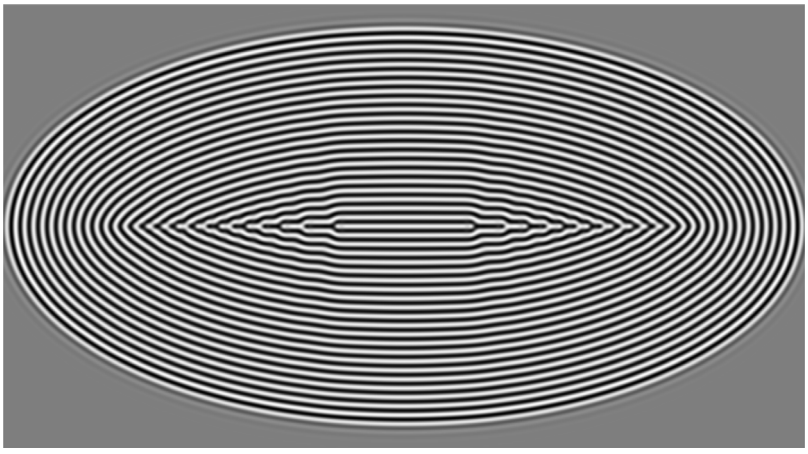

Fig. 6. A numerical simulation of the Swift–Hohenberg equation on an elliptical domain. Compare the eikonal solution on the same domain shown in Fig. 5.

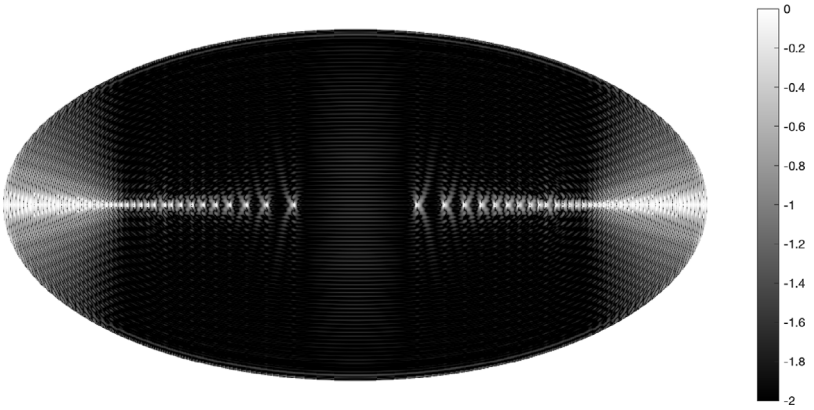

Fig. 7. The grayscale corresponds to $\log_{10}||\nabla\theta| - k_B|$, a measure of the deviation of the local wave-number $|\nabla\theta|$ from the preferred wavenumber $k_B = 1$. The deviation is plotted on a logarithmic scale is for improved contrast. $\| \nabla\theta| - k_B| \lesssim 10^{-2}k_B$ on the bulk of the elliptical domain.

ϵ. Therefore the self-dual approximation will allow for some flattening of phase contours as the major axis is approached. Most of the energy in the pattern, as is clear from Fig. 8, resides along the major axis. This behavior can be approximated by a series of phase contours on the major axis where $\theta = m\pi$ with m integer, and gaps where $\dfrac{\partial\theta}{\partial y} = 0$. Following through with this approach allows us to calculate the optimal placing of the divisions so as to minimize the energy [16]. In all likelihood that will be the multi-dislocation solution (a sum of (3.19) solutions). Another question to address is whether, at the dislocations, one has to reintroduce the amplitude as an additional order parameter as the local wavevector approaches the neutral stability curve where the amplitude is small. In any event, the matching of what is observed, in experiments and in simulations of both the large Prandtl number Oberbeck–Boussinesq equations and its toy model the Swift–Hohenberg equation, provides a healthy but yet unresolved challenge for the theory.

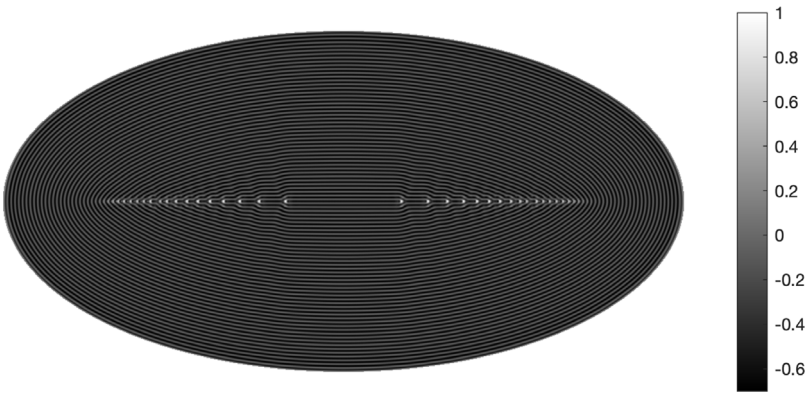

Fig. 8. The local energy density on the Swift–Hohenberg solution on an elliptical domain. The energy density is normalized by its maximum value. As expected, the total energy is negative since the energy of the stripe patterned state is less than that of the homogeneous state.

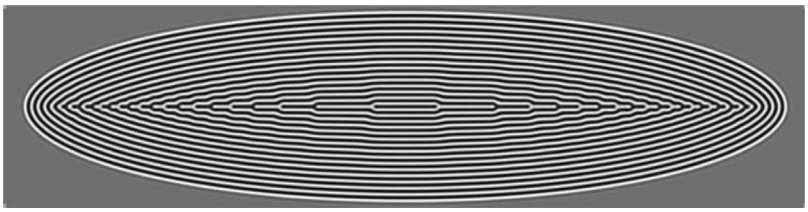

Fig. 9. The Swift–Hohenberg solution on an elliptical domain with a larger aspect ratio.

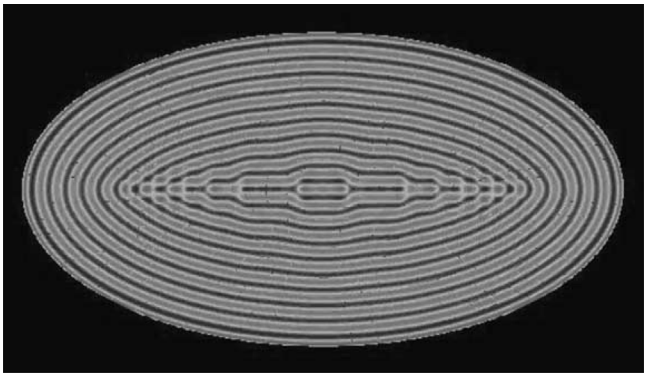

Fig. 10. Numerical simulation of the Oberbeck–Boussinesq equations for convection.

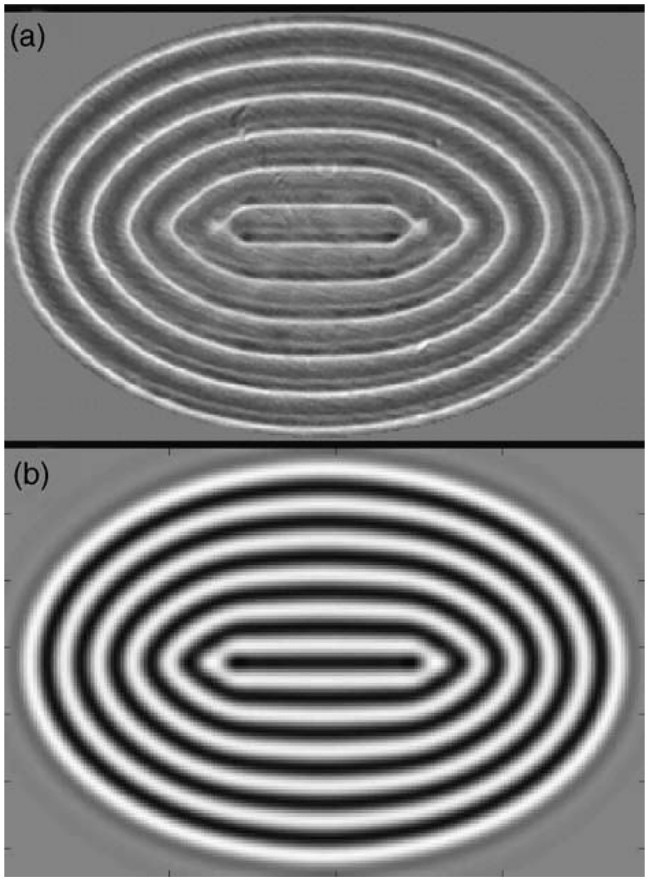

Fig. 11. (a) Experimental results for convection in an elliptical container. (b) Simulation of the Swift–Hohenberg equation on the same domain.

3.2. Pattern quarks and leptons and a second challenge

We saw in 3.1 that the canonical point defects in two-dimensional striped patterns were concave (V) and convex (X) disclinations. Their associated invariants, namely the "Twists", measuring the amount of Gaussian curvature condensed onto the point defects, when divided by 2π were fractional, $-\frac{1}{2}$ and $\frac{1}{2}$ respectively. In three dimensions, the point defect analogs of the *V* and *X* will easily dissociate, while loop defects are stable and encode interesting topology [17]. The defects that are structurally stable are loops (see Figs. 13 and 14) in which the cross-sections are concave and convex disclinations.

As we shall see, they still retain their "spin" or $\pm\frac{1}{2}$ invariants. However, because the tori that envelope these loops have two

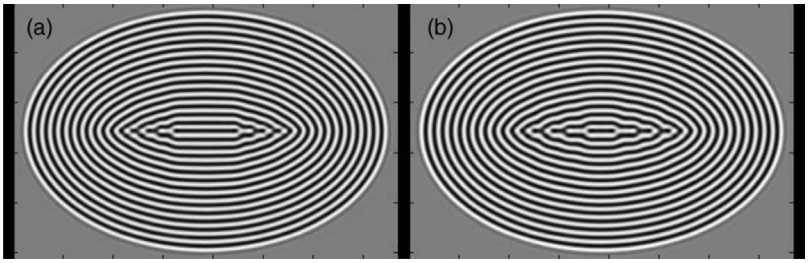

Fig. 12. Simulations of the Swift–Hohenberg equation. Note the flattening of the phase contours as the major axis is approached.

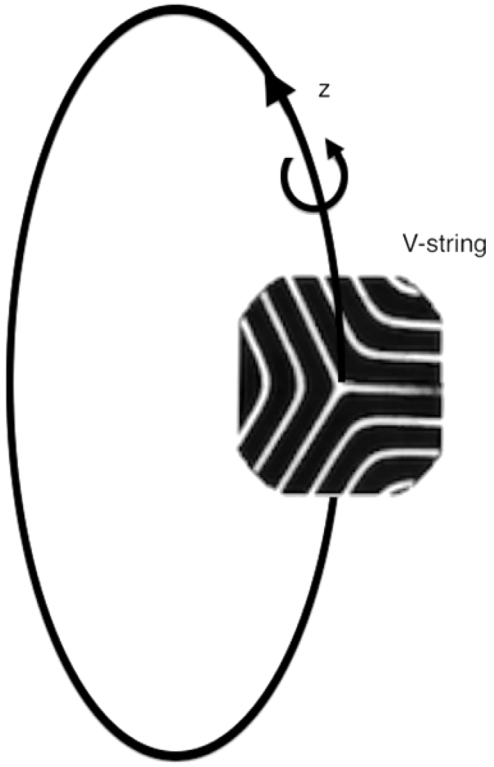

Fig. 13. A phase defect in three dimensions with a concave disclination backbone.

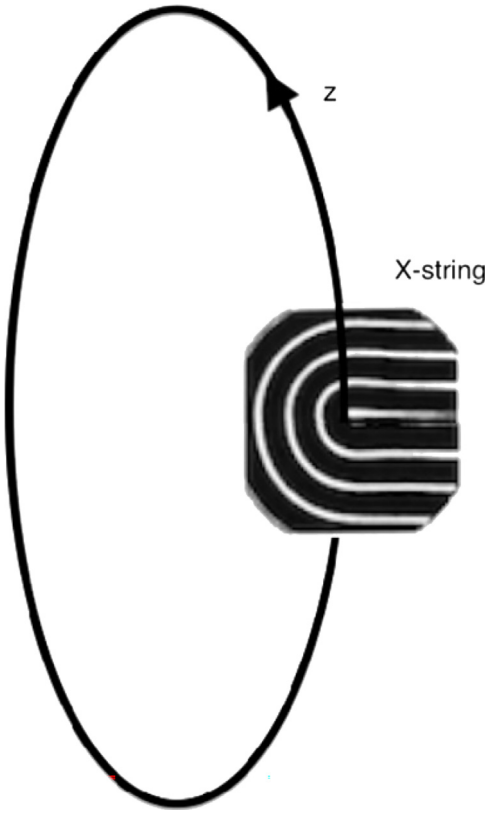

Fig. 14. A phase defect with a convex disclination backbone.

independent closed loops on their surfaces on which the total twists of the $\vec{k}$ director are invariant, each loop defect has an additional invariant which in the case of the V (X) string or loop with a concave (convex) disclination cross-section, can be integer multiples of $\frac{1}{3}$ (1). Because of the analogy with the corresponding electric charges, we call these objects pattern quarks and leptons [18].

Before we give the results of these calculations, we point out that the main ideas of the two invariants can be seen from a geometrical viewpoint. For the V string, the object of interest is a loop with a concave disclination cross-section which is twisted about the backbone so as to match the $w(\vec{x}, t)$ field at the two ends $z = 0$ and $z = l$ which are identified. This can be done in essentially two ways. We can ask either that the phase field is periodic, i.e. $\theta(x, y, z = 0) = \theta(x, y, z = l)$ or anti-periodic, i.e. $\theta(x, y, z = 0) = -\theta(x, y, z = l)$. To achieve the former we must match sectors S1 and S3, as shown in Fig. 15, which will require a twist of the direction $f, g, h = \nabla\theta$ along a suitable contour joining $r = r_0, \alpha = 0, z = 0$ to $r = r_0, \alpha = \frac{4\pi}{3}, z = l$ of $\frac{2}{3} \cdot 2\pi$.

To achieve the latter, we simply match sectors of S1 and S2 which will require an angular twist of $\frac{1}{3} \cdot 2\pi$. Each of their negatives is also possible by twisting in the clockwise direction. The spin invariant is obtained by examining the twist of the direction $\nabla\theta$ around any cross-section. For the X-string, the field $w(\vec{x}, t)$ can only be made periodic in the backbone direction by twisting the backbone by an integer multiple of 2π. The spin index again is $\frac{1}{2}$. To envision these invariants, consider a torus containing each loop defect shown in Figs. 13 and 14. There are two independent contours (the generators of the Homology group H_1) on the torus along which one can compute the net twist of the director field. Each invariant is associated with the twist of the director field around the two independent generators on the torus and the line integrals can be related to the area integrals of the two independent and nontrivial sectional Gaussian surface curvatures of the three-dimensional surface $\theta(x, y, z)$.

It is worth remarking on and emphasizing this extraordinary possibility. We start from a field evolving under dynamics imbued with only rotational and translational symmetry. However, when

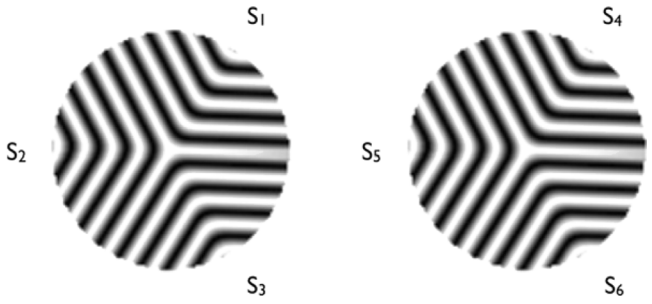

Fig. 15. Concave disclinations and fractional twist.

sufficient stress is applied to that system, there naturally emerge objects with fractional invariants. Contrast this with the standard model (TSM) of theoretical physics in which, informed by the experiments of the early seventies, the symmetries associated with $U(1)$, $SU(2)$, and $SU(3)$ were invoked to capture the charge and spin invariants associated with quarks and leptons. In the context of patterns, there is no imposition of such symmetries *a priori*. The stress on the system causes instabilities, and the melding of differently oriented planar stripe patterns leads to loop defects with precisely the fractional invariants associated with charge and spin.

Here is an outline of what we wish to present. We begin with a listing of previous results although now fortified by our understanding that, even in three dimensions, the self-dual approximation is valid. To simplify the formulae, we choose units such that β and k_B are both unity. We then pose a series of outstanding challenges.

It is a useful exercise to employ what we call the Laplacian approximation to consider solution to the phase diffusion equation in the special case where we take $B(\vec{k}) \equiv 1$ and satisfy each of its two terms separately by solving $\nabla \cdot \vec{k} = \nabla^2\theta = 0$. Since $\nabla \times \vec{k}$ is also zero, in two dimensions this means that $f_x = -g_y, f_y = g_x$ which are the Cauchy–Riemann conditions guaranteeing that $f - ig$ is analytic in $x + iy$.

Disinclinations are captured by the functions $z^{1/2}$ and $\frac{1}{z^{1/2}}$ analytic on the Riemann surface which is the double cover of the plane. Indeed such singularities arise in the theory of quadratic diffentials. Choose $\theta(x,y) = \mathrm{Im}\frac{2}{3}\zeta^{3/2}, \zeta = x + iy, = \rho^{3/2}\sin(\frac{3\alpha}{2})$ where $(x,y) = (\rho\cos(\alpha), \rho\sin(\alpha))$. A little analysis shows $f - ig = \rho^{1/2}\exp(\frac{i\alpha}{2}) = ke^{-i\varphi}$ where $(f,g) = (k\cos\varphi, k\sin\varphi)$ Then $\varphi = -\frac{\alpha}{2}$. As α travels around the defect at $\zeta = 0$, the corresponding twists in φ is $-\pi$. This is the two dimensional Laplace or harmonic concave disclination. The Laplace convex disclination is found by choosing $\theta = \mathrm{Im}(2\zeta^{1/2})$. In three dimensions, we solve Laplace's equation on a cylinder with a backbone along the z–axis identifying $\theta(x,y,0)$ with $\theta(x,y,l)$ in various ways described earlier when we discussed the main ideas.

For the V-string, or pattern quarks, the Laplacian approximation can be written as

$$\theta = \frac{2}{3}Kr^{\frac{3}{2}}\sin\left(\frac{3\alpha}{2} - \frac{n\pi z}{l}\right) \tag{3.20}$$

where n is integer and we have approximated the Bessel function $I_{\frac{3}{2}}(r)$ by its small argument limit. Therefore we work in the radial domain $2\pi(=\lambda) \ll r \ll l$.

$$f - ig = Kr^{1/2}\exp i\left(\frac{\alpha}{2} - \frac{n\pi z}{l} - \frac{\pi}{2}\right) \tag{3.21}$$

$$h = -\frac{2\pi n}{3l}Kr^{3/2}\cos\left(\frac{3\alpha}{2} - \frac{n\pi z}{l}\right) \tag{3.22}$$

We note that, for $\frac{r}{l}$ small, $|h| \ll |f|, |g|$. Therefore the twist of the direction (f,g,h) can be calculated from the change in ϕ where $f - ig = \sqrt{f^2+g^2}\exp(-i\varphi)$, $\sqrt{f^2+g^2} = Kr^{1/2}$.

$$\varphi = -\frac{\alpha}{2} + \frac{n\pi z}{l} + \frac{\pi}{2} \tag{3.23}$$

Along the contour $z = $ constant, $0 \le \alpha \le 2\pi$, the twist or change in ϕ is $-\pi$. Along the contour $\alpha = \alpha_0 + \frac{2\pi}{3}t, z = \frac{l}{n}t, r = r_0(\alpha_0), 0 \le t \le n$ on which θ and h are constants, the change of φ, $\frac{1}{2\pi}[\varphi]$ is

$$\frac{1}{2\pi}[\varphi] = \frac{1}{3}n. \tag{3.24}$$

For θ periodic over $0 \le z \le l$, n is even and its smallest value is $n = 2$. We call this the pattern up quark. For θ antiperiodic, we choose $n = 1$. We call this the pattern down quark. The corresponding index is $\frac{1}{3}$. For X-strings, or pattern leptons, the Laplace solution is $\theta = 2Kr^{1/2}\sin(\frac{\alpha}{2} - \frac{\pi nz}{l})$ for which $f - ig = \sqrt{f^2+g^2}\exp(-i\varphi) = Kr^{1/2}\exp i(-\frac{\alpha}{2} - \frac{\pi nz}{l} - \frac{\pi}{2}), h = -\frac{2nK\pi r^{3/2}}{l}\cos(\frac{\alpha}{2} - \frac{\pi nz}{l})$. The twist angle is

$$\varphi = \frac{\alpha}{2} + \frac{n\pi z}{l} + \frac{\pi}{2} \tag{3.25}$$

Around the two circuits $r = r_0, z = $ constant, $0 \le \alpha \le 2\pi$ and $r = r_0, z = \frac{l}{n}t, \alpha = \alpha_0 - 2\pi t, 0 \le t \le n$ the respective twists are π and $-2\pi n$. The choice of antiperiodic θ leads to indices ± 1. We note that the choice θ periodic leads to indices ± 2.

We now turn to the self dual problem for which solutions for $\theta(x,y,z)$ are obtained by solving (3.15), the Helmholz equation for ψ and then calculating $\theta = s\ln\psi$.

For the V-string, or pattern quarks, the self dual approximation gives

$$\begin{aligned}\theta_1(r,\alpha,z;n) = {} & \frac{\sqrt{3}}{2}r\cos\left(\alpha - \frac{2n\pi}{3}\frac{z}{l} - \frac{\pi}{3}\right) \\ & - \ln\left(2\cosh\frac{r}{2}\sin\left(\alpha - \frac{2n\pi}{3}\frac{z}{l} - \frac{\pi}{3}\right)\right)\end{aligned} \tag{3.26}$$

$$\begin{aligned}\theta_2(r,\alpha,z;n) = {} & -\frac{\sqrt{3}}{2}r\cos\left(\alpha - \frac{2n\pi}{3}\frac{z}{l} - \pi\right) \\ & + \ln\left(2\cosh\frac{r}{2}\sin\left(\alpha - \frac{2n\pi}{3}\frac{z}{l} - \pi\right)\right)\end{aligned} \tag{3.27}$$

$$\begin{aligned}\theta_3(r,\alpha,z;n) = {} & \frac{\sqrt{3}}{2}r\cos\left(\alpha - \frac{2n\pi}{3}\frac{z}{l} - \frac{5\pi}{3}\right) \\ & - \ln\left(2\cosh\frac{r}{2}\sin\left(\alpha - \frac{2n\pi}{3}\frac{z}{l} - \frac{5\pi}{3}\right)\right)\end{aligned} \tag{3.28}$$

The sectors are rotated versions of those shown in Fig. 15 and are defined by $\frac{2(n-1)}{3}\pi < \alpha - \frac{2n\pi}{3}\frac{z}{l} < \frac{2n\pi}{3}, n = 1-6$. The solutions are approximate, valid for $2\pi \ll r \ll l$. The phase functions $\theta_4, \theta_5, \theta_6$ in sectors 4, 5, 6 are the negatives of those in S1, S2, S3. The z dependence of the arguments are chosen so that, under the twist associated with integer n, the points α_0 on $z = 0$ rotate to $\alpha_0 + \frac{2n\pi}{3}$ on $z = l$. We note that

$$\theta_1(r,\alpha,z=l;n=2) = \theta_3(r,\alpha,z=0;n=2) \tag{3.29}$$

and

$$\theta_1(r,\alpha,z=l;n=1) = -\theta_2(r,\alpha,z=0;n=1). \tag{3.30}$$

In the first case, we match sectors 1 and 3. The twist along the helical contour joining $(r_0, 0, 0)$ to $(r_0, \frac{4\pi}{3}, l)$ is $\frac{4\pi}{3}$. In the second case, the twist is $\frac{2\pi}{3}$. Again the twist along a contour at constant z is $-\pi$. A similar three dimensional analogue to the two dimensional solutions gives twists for the X-string of π and $-2\pi n$.

There is a connection of the "charge" invariants with the Gaussian curvature of the twisting phase surface that has a boundary which consists of C1: a helical curve joining $(r = r_0, \alpha = 0, z = 0)$ to $(r = r_0, \alpha = \frac{4\pi}{3}, z = l)$; C2: the straight line at $\alpha = \frac{4\pi}{3}$, joining $r = r_0$ to $r = 0$; C3 : the backbone on which $k \to 0$ joining $z = l$ to $z = 0$ at $r = 0$; and C4 : The straight line joining $r = 0, \alpha = 0, z = 0$ to $r = r_0, \alpha = 0, z = 0$. The value of $\frac{1}{2\pi}\int_{C_1} k^2 d\varphi$ is $\frac{2}{3}$. Its value on C2 and C4 is zero because on these straight lines $[\phi] = 0$. The value along the backbone is also zero. Thus $\frac{1}{2\pi r_0} \cdot 2\int(\nabla f \times \nabla g)\cdot \hat{n} dS$ which adds the projections of $(\nabla f \times \nabla g)$ onto $z = 0, r \le r_0, 0 \le \alpha \le \frac{4\pi}{3}$ and onto $\alpha = 0, 0 \le r \le r_0, 0 \le z \le l$ is $\frac{2}{3}$. One can calculate these integrals for the case where we approximate θ by $\frac{2}{3} r \frac{3}{2} \sin(\frac{3\alpha}{2} - \frac{2\pi z}{l})$. Then $\frac{1}{4}(f_r g_\alpha - f_\alpha g_r) = -\frac{1}{4r}, f_r g_z - f_z g_r = \frac{\pi}{l}$ and $\frac{1}{r}(f_\alpha g_z - f_z g_\alpha) = 0$. The integral $\frac{2}{2\pi r_0}\int_0^{r_0}\int_0^{\frac{4\pi}{3}} \frac{1}{r}(f_r g_\alpha - f_\alpha g_r) r dr d\alpha = -\frac{1}{3}$ whereas $\frac{2}{2\pi r_0}\int_0^{r_0}\int_0^{l} \frac{\pi}{l} dr dz = 1$.

In the harmonic case, one must divide out by the radius r_0 as the wavenumber does not tend to 1 (the non-dimensional k_B) in the far field but to r. Therefore the two sets of invariants, the "spins", $-\frac{1}{2}$ and $\frac{1}{2}$, and the "charges" $\pm 1, \pm\frac{2}{3}, \pm\frac{1}{3}$, reflect the amounts of sectional Gaussian curvatures which have condensed on the loop backbones. On the other hand, the energy of the V string is proportional to the mean curvature condensed along the PGBs for the V-string which is proportional to $3\sin^3\frac{\pi}{6}$ multiplied by the product of its cross sectional and backbone lengths L and l. The X-string energy is proportional to $l \ln L$.

There are several open challenges. Most are of interest in their own right and aim at gaining a better understanding of the defects contained in natural patterns. Others are motivated by the possibility of connections with the origins of subatomic particles.

1. The embedding of disclinations in physically reasonable far fields. Even in two dimensions, this is a challenge. Our calculations of the energy of the concave disclination assume that the three phase grain boundaries have infinite extent. So this brings up the question: Are disclinations finite in size with finite energy and, if so, how do the contributions from the phase grain boundaries (discontinuities in the gradient of the phase field) in the case of the concave disclination and of discontinuities in second derivative (curvature) in the case of convex disclinations decay as r, the distance from the core, increases and how do these objects meld in with physically reasonable far fields? Perhaps they do not. Perhaps they are part of a very slowly coarsening process which only ends after many mergings and when the final defect configuration is of the size of the system and constrained from complete elimination only by boundary constraints. These questions become even more difficult when we consider the V and X strings in three dimensions. Can they be embedded in $\mathbb{R}^3$ or do they require the notion of a wrapped up dimension so that the configuration space is not $\mathbb{R}^3$ but $S^1 \times \mathbb{R}^2$ or more simply a torus?
One can try to think of gedanken experiments. In [11], we showed how a striped convective pattern evolves in an elliptical cylinder whose sidewalls are heated. Near the boundary, the convection rolls are parallel to the walls (their wavevector $\vec{k}$ is normal to the wall) and their wavelength is the preferred value, the eikonal construction. But the normals to an elliptical cylinder form caustics emanating from the two foci so that the eikonal solution leads to multivaluedness. A thin film elastic blister would regularize this solution by introducing a wedge-like boundary roof layer between the two foci and allow for a discontinuity (PGB) in the gradient of the height [11]. The angle α between the wavevector and the PGB is zero at both foci and increases towards the center. What we find in a convecting fluid is that, once $\alpha > 43^\circ$, the pattern develops non-orientable defects resulting from director field perturbations of what was previously a vectorfield. There is a creation of VX pairs, a nipple instability, and a prediction supported by both numerical and experimental confirmations, the former using both the Swift–Hohenberg approximations and the full Oberbeck–Boussinesq equations. The final pattern (presumably the energy minimum although, for nonconvex problems, one has no uniqueness result; in some circumstances, one can show by finding almost coincident upper and lower bounds [19] that an observed configuration has an energy that the minimum must have) consists of what appears to be a chain of "dislocations" in which $\nabla\theta\cdot\hat{n}$ and θ mod π are both zero on alternating segments on the chain axis [16]. The number is determined by the aspect ratio of the elliptical container. In an experiment conducted by Ahlers and colleagues [14] there is only one defect (See Fig. 11(a)). It would be interesting to attempt an experiment in an ellipsoidal container, axisymmetric around its long axis, with some pattern producing system, possibly chemical in nature, which can produce three dimensional patterns. One might conjecture that one would obtain a bound zero charge pair of VX strings because there is no twist along the backbones. It might be also possible to use a toroidal cylinder with elliptical cross section in which one might induce a 2π twist, a hydrogen atom like arrangement.
2. **Interstring forces**. Whereas much is known about the interaction energies and forces between vortices (a back to back superposition of two convex disclinations) and dislocations (two concave, two convex dislocations) in vectorfield pattern forming systems, and, in certain cases, between disclinations in two dimensions, nothing is yet known about the interaction forces between loop disclinations. Some of the difficulty is that we do not have finite energies for individual disclinations. What one would like to be able is to calculate the interaction free energy between two such objects by renormalizing, i.e. subtracting the individual free energies from that of the combination and calculating its dependence on the parameters r, an appropriate choice of interdisclination distance, and the spin and charge indices. An alternative approach might follow the framework introduced in [20] to effect the renormalization by introducing additional "defect"-fields that modify the energy functional to keep it finite even

in the presence of disclinations. One would like to see whether, for example, the renormalized interaction energy between a single V-string with 2π twist (two up quarks and one down quark) and an X string is proportional to the product of the signed charges and inversely proportional to r, the separation between the strings.

3. **Composites of pattern quarks and leptons**. A related question concerns the composition of pattern quarks and leptons. Presumably one cannot match an individual up or down pattern quark with a pattern lepton because their charges (which are related to their topological structures) do not match. Therefore, one might conjecture that if pattern quarks and leptons can only appear (stably) in pairs then we require quark composites whose indices add to multiples of ± 1, e.g. two up quarks and a negative down quark (a pattern proton). One could also add a zero charge configuration, e.g., integer multiples of one up and two down quarks (a pattern neutron). Do such composites consist of pattern up and down quarks which share the same loop backbone (and whose topologies are clearly calculated by the addition of indices) or can one have interlinked loops? We should note that their cousins in excitable media, vortices with vectorfield order parameters, tend to appear as single rather than interlinked loops.
4. **More sophisticated models**. Patterns can arise as stationary (exchange of stabilities) or as traveling or standing waves (overstability). The latter arise when the unstressed system supports oscillatory or wave motion. For example, the next most simple model of atmospheric motion is the beta plane model which adds the north–south dependence of Coriolis parameter to the geostrophic balance. When stressed with a north–south temperature gradient, the resulting vertical shear of the east–west velocity and associated density, pressure fields can destabilize via what is called the baroclinic instability to a traveling pattern which has the character of Rossby waves, the natural oscillations of the unstressed system. Therefore the recipe for a pattern forming system with waves is a superposition of Hamiltonian and gradient flows. It would be interesting to investigate the nature of defects in a pattern forming system whose Hamiltonian component had Lorenz symmetry added to that of translation and rotation. The system is stressed by the addition of the gradient component.

Declaration of competing interest

The authors declare that they have no known competing financial interests or personal relationships that could have appeared to influence the work reported in this paper.

Data availability

Data will be made available on request.

Acknowledgments

We are also grateful to the two referees for a careful reading of the manuscript and their thoughtful comments, which significantly improved the paper. The authors of this work were supported by the award NSF-GCR 2021019. SCV was also supported in part by NSF-DMR 1923922.

References

[1] M.C. Cross, P.C. Hohenberg, Pattern formation outside of equilibrium, Rev. Modern Phys. 65 (1993) 851–1112.
[2] S. Chandrasekhar, Hydrodynamic and Hydromagnetic Stability, in: International Series of Monographs on Physics, Clarendon Press, 1961.
[3] Joseph B. Keller, Perturbation theory of nonlinear wave propagation, J. Acoust. Soc. Am. 54 (1) (2022) 325, 06/27 1973.
[4] G.B. Whitham, Linear and nonlinear waves, Wiley-Interscience [John Wiley & Sons], New York-London-Sydney, 1974, Pure and Applied Mathematics.
[5] M.C. Cross, Alan C. Newell, Convection patterns in large aspect ratio systems, Physica D 10 (3) (1984) 299–328.
[6] T. Passot, A.C. Newell, Towards a universal theory for natural patterns, Physica D 74 (3–4) (1994) 301–352.
[7] Y. Pomeau, P. Manneville, Stability and fluctuations of a spatially periodic convective flow, J. de Phys. Lett. 40 (23) (1979) 609–612.
[8] Alan C. Newell, J.A. Whitehead, Finite bandwidth, finite amplitude convection, J. Fluid Mech. 38 (2) (1969) 279–303.
[9] Lee A. Segel, Distant side-walls cause slow amplitude modulation of cellular convection, J. Fluid Mech. 38 (1) (1969) 203–224.
[10] J. Swift, P.C. Hohenberg, Hydrodynamic fluctuations at convective instability, Phys. Rev. A 15 (1) (1977) 319–328.
[11] A.C. Newell, T. Passot, C. Bowman, N. Ercolani, R. Indik, Defects are weak and self-dual solutions of the Cross-Newell phase diffusion equation for natural patterns, Physica D 97 (1) (1996) 185–205.
[12] Patricio Aviles, Yoshikazu Giga, A mathematical problem related to the physical theory of liquid crystal configurations, in: Miniconference on Geometry and Partial Differential Equations, 2 (Canberra, 1986), in: Proc. Centre Math. Anal. Austral. Nat. Univ., vol. 12, Austral. Nat. Univ., Canberra, 1987, pp. 1–16.
[13] A.A. Nepomnyashcy, L.M. Pismen, Singular solutions of the nonlinear phase equation in pattern-forming systems, Phys. Lett. A 153 (8) (1991) 427–430.
[14] Worawat Meevasana, Guenter Ahlers, Rayleigh-Bénard convection in elliptic and stadium-shaped containers, Phys. Rev. E 66 (2002) 046308.
[15] N. Ercolani, R. Indik, A.C. Newell, T. Passot, Global description of patterns far from onset: A case study, Physica D 184 (1) (2003) 127–140.
[16] N.M. Ercolani, S.C. Venkataramani, A variational theory for point defects in patterns, J. Nonlinear Sci. 19 (3) (2009) 267–300.
[17] Thomas Machon, Hillel Aharoni, Yichen Hu, Randall D. Kamien, Aspects of defect topology in smectic liquid crystals, Comm. Math. Phys. 372 (2) (2019) 525–542.
[18] Alan C. Newell, 'Quarks' and 'leptons' in three dimensional patterns, Eur. J. Mech. B/Fluids 47 (2014) 39–47.
[19] Peter Sternberg, The effect of a singular perturbation on nonconvex variational problems, Arch. Ration. Mech. Anal. 101 (3) (1988) 209–260.
[20] Chiqun Zhang, Amit Acharya, Alan C. Newell, Shankar C. Venkataramani, Computing with non-orientable defects: Nematics, smectics and natural patterns, Phys. D: Nonlinear Phenom. 417 (2021) 132828.